Radiation Measurements 177 (2024) 107235

Contents lists available at ScienceDirect

Radiation Measurements

journal homepage: www.elsevier.com/locate/radmeas

Non-monotonic dose dependence of thermoluminescence (TL) revisited

R. Chen [a,*], J.L. Lawless [b], R. Arora [c]

[a] Raymond and Beverly Sackler School of Physics and Astronomy, Tel Aviv University, Tel Aviv, 69978, Israel
[b] Redwood Scientific Incorporated, Pacifica, CA94044-4300, USA
[c] Department of Physics, Punjabi University, Patiala, 147002, Punjab, India

ARTICLE INFO

Keywords:
Thermoluminescence (TL)
Dose dependence
Energy-level model
Simulations

ABSTRACT

The effect of non-monotonic dose dependence of TL intensity on the irradiation dose has been reported in some materials in the past. As opposed to the regular case in which the intensity of the emitted TL light increases monotonically with the applied dose until it reaches saturation, in some reported cases, the light intensity reached a maximum and then declined at higher doses. The effect has been explained by using an energy level model including two electron traps and two hole centers competing with each other, thus yielding the effect. In the present work we show that with the use of certain sets of trap and center parameters, the effect can be seen with a reduced model of one trapping state and two recombination centers. Also, in recent years some experimental results showed more complex non-monotonic dose dependence, namely that following a maximum in the dose-intensity curve, and a certain range of decline, the TL intensity starts to increase again with the dose. We offer a new physical model that may explain this wiggly dose dependence. The energy-level diagram we propose is the same as before, with one electron trap and two kinds of recombination centers, one of which is radiative. In addition, we assume that the high energy radiation can produce more defects in the material which form more radiative recombination centers, this in addition to the filling of new and existing traps and centers by the irradiation. We consider the simultaneous differential equations governing the processes during irradiation, relaxation and heating with the variable dose-dependent concentration of the radiative recombination centers. We solve the equations numerically and by an analytical way with plausible approximations. The wiggly dose dependence results with certain sets of the relevant parameters.

1. Introduction

The dose-dependence curve of thermoluminescence (TL) intensity is usually a monotonically increasing function which, ideally starts linearly. In many cases, at higher doses the curve gets sublinear when the TL maximum intensity approaches saturation. At high doses, the intensity usually approaches saturation which is explained to be the result of trapping states and/or recombination centers being filled to capacity so that further irradiation does not contribute anymore to additional increase in the measured TL.

Rather early in the study of TL, an effect of non-monotonic dose dependence has been found in several materials and following different irradiations. After the TL intensity reached a maximum, at higher doses, the intensity reduced so that the dose dependence curve had a peak-shaped form.

The first researchers who reported the effect were Charlesby and Partridge (1963) who described a decline of the maximum TL intensity in gamma-irradiated polyethylene as of 10^4 Gy, and postulated that the cause of the effect is radiation damage of the material. Halperin and Chen (1966) reported on UV excited TL in semiconducting diamonds and showed that the secondary peak at ~150 K increased linearly with the dose at low doses of UV, reached a maximum at a certain dose and decreased at higher doses. Cameron et al. (1968) described the non-monotonic dose dependence of TL in LiF:Mg,Ti on ^{60}Co gamma-ray excitation dose. In this material which has been serving for many years as the main dosimetric material, the authors report on a rather broad range of linear dependence followed by a superlinear range after which, a maximum value and a slight decline are observed. The effect of non-monotonic dose dependence has also been seen in quartz, the main material used for archaeological and geological TL dating. Ichikawa (1968) found that in gamma-irradiated natural quartz, the peak at ~220 °C reached a maximum at ~6×10^4 Gy and decreased at higher doses by a factor of ~2.5. The effect has also been seen in the important dosimetric material Al_2O_3:C. Yukihara et al. (2003) described slightly

* Corresponding author.
E-mail address: chenr@tau.ac.il (R. Chen).

https://doi.org/10.1016/j.radmeas.2024.107235
Received 26 March 2024; Received in revised form 12 July 2024; Accepted 13 July 2024
Available online 17 July 2024

superlinear dose dependence up to ~30 Gy of beta irradiation in the 450 K peak in some of the samples. The peak reached a maximum value and declined at higher doses. The authors explain the observed effect in Al_2O_3:C using a model based on the occurrence of F/F^+ centers and on the other trapping states and centers. Also reported on the effect in Al_2O_3:C Zahefidar et al. (2012).

More recent reports on this effect in different materials and various irradiations include Sharma et al. (2018), Bargat et al. (2020), Parauha and Dhoble (2020) and Prabhu et al. (2020).

Lawless et al. (2005) and Chen et al. (2006) presented a model for explaining the non-monotonic effect of TL by using an energy-level model including two trapping states and two recombination centers and showed by simulation the feasibility of getting the effect. In a similar way, Pagonis et al. (2006) have shown that the effect can be explained in the measurement of optically stimulated luminescence (OSL). In a quite recent paper, Merezhnikov and Nikiforov (2021) have provided an alternative explanation leading to the non-monotonic behavior of TL, based on the semi-localized transitions (SLT) model.

In this work, we concentrate on less common non-monotonic dose dependence, namely a dose dependence which begins like the "conventional" non-monotonic behavior. The TL intensity starts as an increasing function of the dose, reaches a maximum value and then declines. At a certain higher dose of irradiation, the curve starts increasing again, giving the whole curve a wiggly shape.

Lewandowski and Mathur (1996) report on this effect in γ-irradiated $CaSO_4$ (see their Fig. 1(b)). Mathur et al. (1999) report the effect in proton irradiated $CaSO_4$:Dy (see their Fig. 4). Sharma et al. (2010) present an even more wiggly dose-dependence curve of two TL peaks in CaSrS:Ce (see their Fig. 6). Kortov (2014) report on the wiggly dose dependence in TLD-500 (Al_2O_3:C) detectors at high dose γ-irradiation and more results along the same line were given by Kortov et al. (2015).

Results of the sister-effect of optically stimulated luminescence (OSL) have been reported by Burbidge et al. (2009) who had studied the dose response in α and β excited samples. Different types of dose dependence have been found in quartz samples including non-monotonic and wiggly-shaped cases (Burbidge et al., 2011). The different types of dose dependence have been summed up in a paper by Burbidge, (2015) who, by using the two-trap-two-center model, assembled a function which could describe a range of dose dependencies, namely, linear, superlinear and non-monotonic as well as relative response to α and β radiation. A similar effect in OSL has been described by Kalnins et al. (2012) who had studied radiation dosimetry in fluoride phosphate optical fibers.

In the present work, we deal with two subjects related to the non-monotonic dose dependence. First, we demonstrate, using both numerical solution of the set of coupled differential equations governing the process and by analytical solution with simplifying assumptions, that with the appropriate choice of the relevant parameters of traps and centers, a model of two traps and a single recombination center suffices to explain the conventional non-monotonic dose dependence of TL. As for the explanation of the wiggly dose dependence curve, we add the following crucial element. Whereas the previous models dealt only with transitions of electrons and holes between existing imperfections associated with energy levels in the forbidden gap, we now assume that the high-energy irradiation may produce additional defects that may act as electron or hole traps. More specifically, in the present case, we assume that the luminescent center which we denote by M_2 has prior to irradiation a value of M_{20} and during irradiation more centers of the same kind are created proportionally to the dose of excitation, which brings about the wiggly behavior. Such a wiggly dose dependence can also be demonstrated if at the beginning of irradiation there are no centers of the relevant type, which means that $M_{20} = 0$. The details of the model and the resulting simulated dose dependence are elaborated upon below.

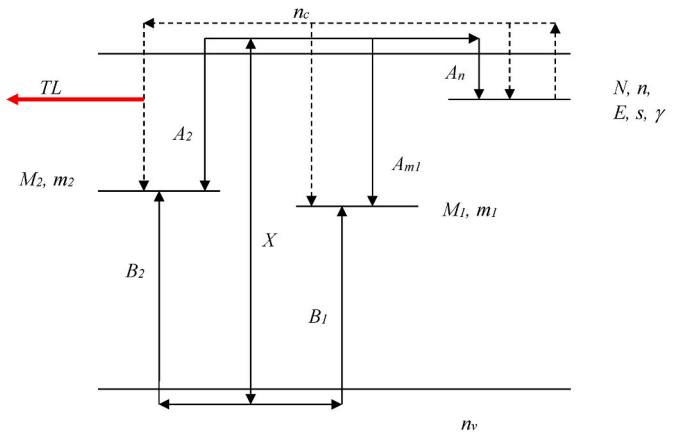

Fig. 1. Energy-level diagram of the model explaining the effect of non-monotonic dose dependence of TL. The model shows a trap N and two centers, M_1 non-radiative and M_2 radiative. The wiggly behavior is reached when M_2 depends on the irradiation dose. Transitions taking place during excitation are shown as solid lines and those occurring during heating as dashed lines.

2. Theory

The energy-level model we use is of one electron trap and two kinds of recombination centers as depicted in Fig. 1. For the conventional non-monotonic dose dependence we will show that the model can explain this dependence with the appropriate choice of the parameters of traps and centers. As pointed out above and shown below, we demonstrate that if we assume that the concentration M_2 grows linearly with the dose of irradiation, the wiggly-shaped dose dependence may result. Two examples will be considered, namely, $M_2(t) = M_{20}+at$ with $a>0$, one with $M_{20} > 0$ and the other with $M_{20} = 0$. In the mentioned simpler case of conventional non-monotonic dose dependence we assume that $a = 0$ so that M_2 is constant, M_{20}.

2.1. Governing equations

The model uses one electron trap and two recombination centers. The governing equations are

$$\frac{dn}{dt} = A_n(N-n)n_c - \gamma n, \tag{1}$$

$$\frac{dm_1}{dt} = -A_{m1}m_1n_c + B_1(M_1-m_1)n_v, \tag{2}$$

$$\frac{dm_2}{dt} = -A_{m2}m_2n_c + B_2[M_2(t)-m_2]n_v, \tag{3}$$

$$\frac{dn_c}{dt} = X + \gamma n - A_n(N-n)n_c - A_{m1}m_1n_c - A_{m2}m_2n_c, \tag{4}$$

$$\frac{dn_v}{dt} = X - B_1(M_1-m_1)n_v - B_2[M_2(t)-m_2]n_v, \tag{5}$$

where A_n (m^3s^{-1}) is the rate constant for the capture of an electron by the electron trap, N (m^{-3}) is the total concentration of electron traps, n (m^{-3}) is the instantaneous concentration of occupied traps. Similarly, B_1 (m^3s^{-1}) and B_2 (m^3s^{-1}) are the rate constants for hole capture by the two centers with M_1 (m^{-3}) and $M_2(t)$ (m^{-3}) being the total concentration of those centers and m_1 (m^{-3}) and m_2 (m^{-3}) being the hole concentrations of the occupied centers. A_{m1} (m^3s^{-1}) and A_{m2} (m^3s^{-1}) are the rate constants for free electron recombination with a hole in an occupied center. X ($m^{-3}s^{-1}$) is the rate at which the applied radiation generates electron-hole pairs, which is proportional to the dose rate. n_c (m^{-3}) and n_v (m^{-3}) are, respectively, the instantaneous concentrations of free electrons and free holes. γ (s^{-1}) is the rate constant for thermal stimulation of an electron into the conduction band,

$$\gamma = s\exp(-E/kT), \tag{6}$$

where E (eV) is the trap energy, k (eV/K) is the Boltzmann constant, and T (K) is temperature. Conservation of charge requires

$$n + n_c = m_1 + m_2 + n_v. \tag{7}$$

We will assume that m_1 is a non-radiative center while m_2 is a radiative center. Thus, the thermoluminescence intensity is

$$I = A_{m2} m_2 n_c. \tag{8}$$

Equation (1) through (8) are the governing equations as used by the numerical simulation. We will use the following parameters: $A_n = 3 \times 10^{-17}$ m^{3}s^{-1}; $N = 10^{21}$ m^{-3}; $B_1 = 1.5 \times 10^{-17}$ m^{3}s^{-1}; $B_2 = 10^{-17}$ m^{3}s^{-1}; $A_{m1} = 10^{-17}$ m^{3}s^{-1}; $A_{m2} = 10^{-16}$ m^{3}s^{-1}; M_1=3×10^{21} m^{-3}; $X = 3 \times 10^{19}$ m^{-3}s^{-1}; $s = 10^{10}$ s^{-1} and $E = 1$ eV. For the dose-dependent center concentration we assume an increase with dose according to

$$M_2(t) = 10^{18} + (Xt)/13400 \ \ m^{-3}. \tag{9}$$

For the analytical model, we make additional assumptions regarding m_2, n_c and n_v. First, we will assume that m_2 is 'small'. In particular, we assume that

$$m_2 \ll m_1 \quad and \quad B_2 M_2 \ll B_1 M_1 \quad and \quad A_{m2} m_2 \ll A_{m1} m_1. \tag{10}$$

From Eqs. (4) and (5) and using Eq. (10), the lifetimes (s) of free electrons and holes are

$$t_c = \frac{1}{A_n(N-n) + A_{m1} m_1} \quad and \quad t_v = \frac{1}{B_1(M_1 - m_1)}. \tag{11}$$

Lifetimes of free electrons and holes in materials tend to be quite small, often microseconds or less (Lax, 1960). In quartz, for example, t_c has been experimentally measured to be less then 5 ns (Hughes, 1975). Because the lifetimes are short, there is no chance for populations of free electrons or holes to accumulate. Consequently, n_c and n_v remain small. Further, these lifetimes are short compared to either the period of irradiation or any events that occur during heating. Thus,

$$\frac{dn_c}{dt} \ll \frac{n_c}{t_c} \quad and \quad \frac{dn_v}{dt} \ll \frac{n_v}{t_v}. \tag{12}$$

Under these assumptions, Eqs. (4) and (5) simplify to

$$n_c = \frac{X + \gamma n}{A_n(N-n) + A_{m1} m_1} \quad and \quad n_v = \frac{X}{B_1(M_1 - m_1)}. \tag{13}$$

With n_c, n_v and m_2 being small, conservation of charge, Eq. (7), simplifies to

$$n \approx m_1. \tag{14}$$

In sum, we have started with the general equations for a one-trap two-center model, Eqs. (1) through (8), which are used for the numerical simulation. For the analytical model, we add the additional assumptions of m_2 being small and n_c and n_v being quasi-steady.

3. Analytical model

3.1. Irradiation

In this section, we will develop an analytical model for the concentrations achieved by the trap and centers after irradiation. The irradiation is assumed to occur at a constant rate X for a time period t_D, giving a total dose of D=$X \cdot t_D$. During irradiation, the temperature is assumed low enough that thermal stimulation of trapped electrons, proportional to γ (see Eq. (6)), can be neglected. The initial conditions for irradiation are assumed to be

$$n = m_1 = m_2 = 0. \tag{15}$$

Under these conditions, and using Eq. (13), Eq. (14) and Eq. (10), conservation of trap population simplifies to

$$\frac{dn}{dt} = \frac{A_n(N-n)}{A_n(N-n) + A_{m1} n} X. \tag{16}$$

This equation has an analytical solution (Pagonis et al., 2020; Lawless and Timar-Gabor, 2024). For the present model, the solution can be written as follows. For $A_n \neq A_{m1}$,

$$m_1(t) = n(t) = N\left\{1 + \frac{1}{Q} W\left[-Q\exp\left\{-\left(1 - \frac{e-1}{e}Q\right)(Xt/D_{63\%}) - Q\right\}\right]\right\}, \tag{17a}$$

and on the other hand, for the special case of A_n=A_{m1},

$$m_1(t) = n(t) = N[1 - \exp(-Xt/D_{63\%})], \tag{17b}$$

where e is the base of the natural logarithm, W is the Lambert-W function (Coreless and Jeffrey, 2002)[1] and Q and $D_{63\%}$ are defined by

$$Q = \frac{A_{m1} - A_n}{A_{m1}}, \tag{18}$$

$$D_{63\%} = \frac{A_{m1}}{A_n} N\left[1 - \frac{e-1}{e} Q\right]. \tag{19}$$

For the parameters chosen in this manuscript, $Q \approx -2$ and $D_{63\%} \approx 7.6 \times 10^{20}$ m^{-3}. The negative value of Q indicates that, below saturation, the growth of n with dose is only slightly sublinear. $D_{63\%}$ is the dose at which the trap population, n, starts to approach saturation as signified by $n = \frac{e-1}{e} N \approx 63\% N$.

The next step is to determine the population of the second recombination center, m_2, during irradiation. We can rewrite the conservation equation for m_2, Eq. (3), as follows,

$$\frac{dm_2}{d\tau} = m_{2QS} - m_2, \tag{20}$$

where

$$\tau(t) = \int_0^t (A_{m2} n_c + B_2 n_v) dt, \tag{21}$$

$$m_{2QS}(t) = \left(\frac{B_2 n_v}{A_{m2} n_c + B_2 n_v}\right) M_2(t). \tag{22}$$

τ is dimensionless and can be thought of as a stretched time. m_{2QS} has units of concentration. It is apparent from Eq. (20) that, when $m_2 < m_{2QS}$, m_2 increases. Alternatively, when $m_2 > m_{2QS}$, m_2 decreases. This indicates that m_{2QS} is an attractor.

It is important to note that, because we have solutions for n and m_1 as functions of time, Eq. (17), and because n_c and n_v are known functions of n and m_1, Eq. (13), it follows that τ and m_{2QS} should be regarded as known (or easily calculated) functions of time. With that in mind, Eq. (20) can be readily integrated to find

$$m_2(t) = e^{-\tau(t)} \int_0^{\tau(t)} m_{2QS}(\tau') e^{\tau'} d\tau', \tag{23}$$

where τ' is a variable of integration. Equation (23) indicates that m_2 is zero at $t = 0$ and then grows until it approaches m_{2QS} and eventually attempts to follow the changing values of m_{2QS}.

In sum, under the small-m_2 approximation (see Eq. (10)) we have developed an analytic model of trap and center populations during irradiation. n and m_1 follow Eq. (17) while m_2 obeys Eq. (23). n_c and n_v obey Eq. (13).

[1] The Lambert-W function is defined by $ye^y = x \Rightarrow y = W(x)$. It is supported by major mathematics packages. For SciPi, for example, it is found under **scipy.special.lambertw**.

3.2. Thermal stimulation

The next step is to determine the magnitude of the thermoluminescence intensity. We again start with Eqs. (1)–(5) but this time assume thermal stimulation, namely, $\gamma \neq 0$, but no irradiation, $X = 0$. From Eq. (13), we have $n_v = 0$ and, consequently, the equation for conservation of m_2, Eq. (3) reduces to

$$\frac{dm_2}{dt} = -A_{m2} m_2 n_c. \tag{24}$$

Combining Eq. (24) with Eq. (8), we have for the emitted intensity

$$I = -\frac{dm_2}{dt}. \tag{25}$$

Since $m_2 = 0$ after heating, the integrated thermoluminescence intensity is given by

$$\int_0^\infty I(t)dt = m_2(t_D), \tag{26}$$

where $m_2(t_D)$ is the concentration of m_2 after irradiation as given by Eq. (23).

4. Numerical results

In the numerical results we show first that the conventional non-monotonic dose dependence can be reached by the reduced model of one trapping state and two recombination centers. The set of parameters used is given above with reference to Fig. 1. Figs. 2 and 3 show the results of the trap and centers concentrations and the TL intensity as a function of the excitation dose for a constant value of $M_2 = 10^{18}$ m^{-3}. Fig. 2 shows the dependence of the trapping concentrations as a function of the dose, as determined using the analytical results as well as the direct simulation attained by solving the simultaneous differential equations using the Matlab ode23s solver in the sequence of irradiation, relaxation and heating. Note that with the numerical solutions of the differential equations, there is no need to make the above mentioned simplifying assumptions. Instead, in the results of the numerical solution of the equations, we could check the validity of these simplifying assumptions; the details are given in the Appendix. The results show the initial range of increase of m_2, reaching a maximum and then declining and finally leveling off at a constant value. Fig. 3 shows the dependence on the dose of the integrated emitted TL which resembles the dose-dependence curve of m_2.

In Figs. 4 and 5 we use all the parameters as before and M_2 depending on the irradiation, and show the new wiggly effect where the TL intensity increases up to a maximum, goes down to a minimum and starts increasing again at higher doses. Fig. 4 depicts the results for radiation dependent M_2 as given by Eq. (9). The concentration of m_2 wiggles, reaching a maximum, then a minimum and then it rises again. In Fig. 5, the results of the integrated TL intensity simulated by solution of the coupled equations and by the analytical approach are depicted. Fig. 6 is another example of the simulated dose dependence of TL, this time when the initial concentration of M_2 prior to irradiation is zero, namely,

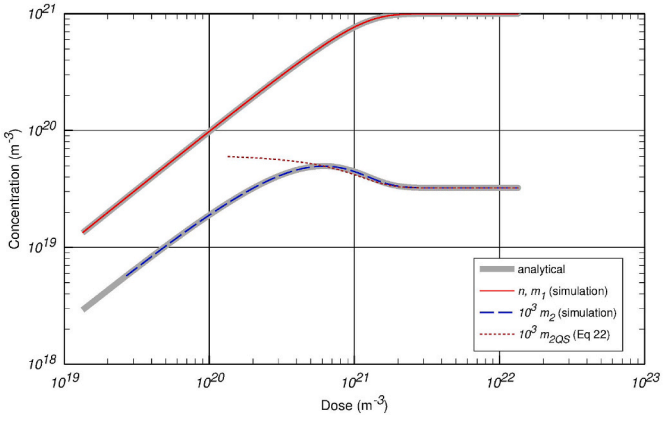

Fig. 2. Results of the concentrations of the trap and centers for constant M_2 as a function of the dose as computed by solving the differential equations and by the analytic approach. The values of the chosen parameters are given in the text.

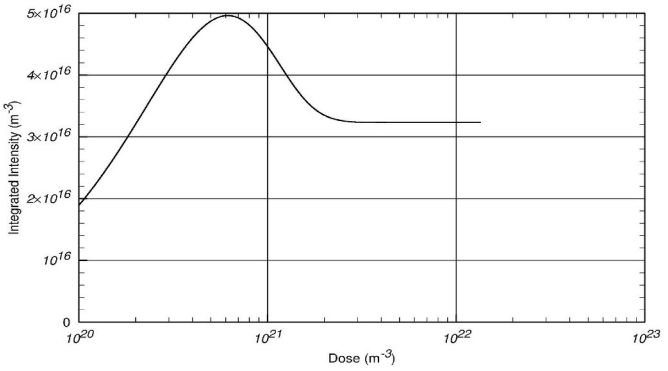

Fig. 3. The dependence of the integrated TL intensity on the dose as determined by the solution of the equations under the same conditions as in Fig. 2.

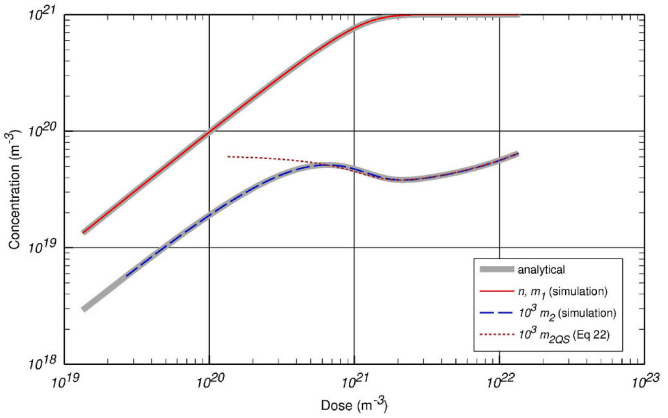

Fig. 4. Calculated values of the concentrations of electrons and holes in traps and centers as function of the dose with the same parameters except that M_2 depends on the dose, varied by different times of excitation according to Eq. (9).

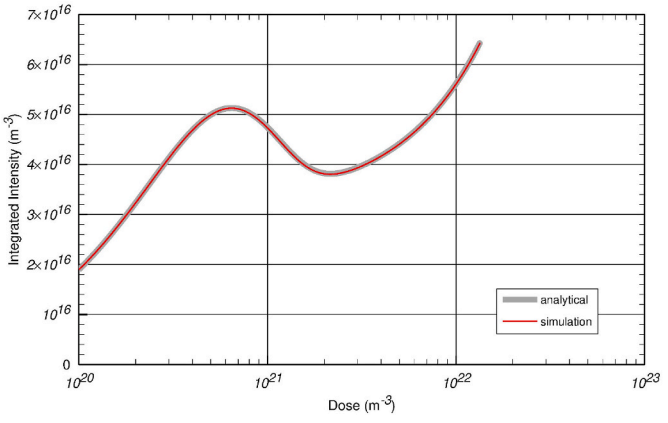

Fig. 5. The TL intensity as a function of the dose as evaluated under the same conditions as in Fig. 4.

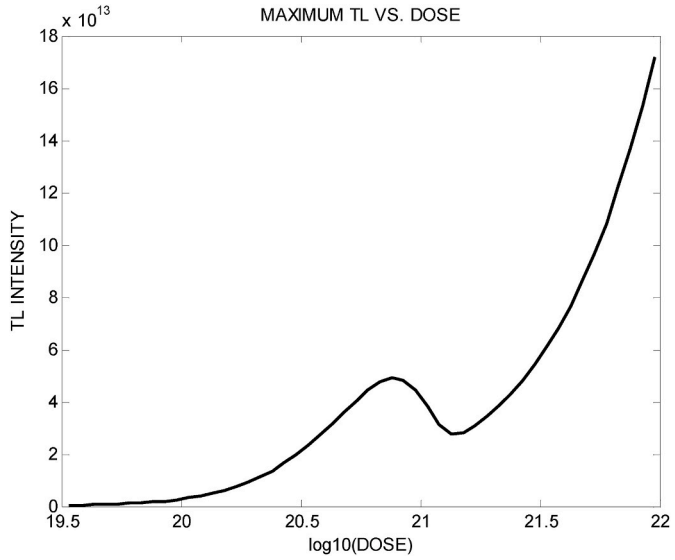

Fig. 6. Similar to Fig. 5, except that the dose dependence of the center concentration, M_2, is as given by Eq. (27).

$$M_2 = 2.24 * 10^{15} t. \quad (27)$$

The dose has been varied by keeping a constant dose rate $X = 3 \times 10^{19}$ m^{-3}s^{-1} and varying the time of irradiation between 1 and 300 s. Here we see a similar wiggly dose dependence for a case of zero initial concentration of the radiative center, $M_2(0) = 0$. It should be mentioned that practically the same results were reached when the time of excitation was kept constant and the dose was changed by varying the dose rate in both cases, namely, when M_2 varied according to Eq. (9) or (27). In this case, the variation of the concentration of the radiative center was given by $M_2(X)$ and X varied linearly between 3×10^{19} m^{-3}s^{-1} and 9×10^{21} m^{-3}s^{-1} and $t_D = 1$ s.

We could also show that the wiggly dose dependence can be reached with different ratios between M_1 and M_2 (t) as demonstrated in Fig. 7 on a log-log scale. M_1 remains the same as before being 3×10^{21} m^{-3}, and M_2(t) is the function given in Eq. (9) in curve (a), 10 times the function in curve (b), 100 times the M_2(t) function in curve (c) and 1000 times the function in curve (d). As seen in the figure, the wiggly dose dependence occurs in all four cases.

5. Discussion

The wiggly dose response can be understood intuitively in relation to changes in the free electron concentration during irradiation. We will discuss this behavior for both the case of constant M_2 and the case of M_2 increasing with dose. This discussion will highlight some of the parameter values that are needed to obtain this behavior. Lastly, for comparison with experiment, the conversion between dose in m^{-3} and dose in Grays will be discussed.

Starting with the case of constant M_2, consider the concentrations of the electron trap, n, and of the non–radiative center, m_1. Since this is a one–trap, two–center model and since the second center, m_2, is considered small (see Eq. (10)), it follows that n and m_1 grow just like in a one-trap, one-recombination-center (OTOR) model. This means that n grows

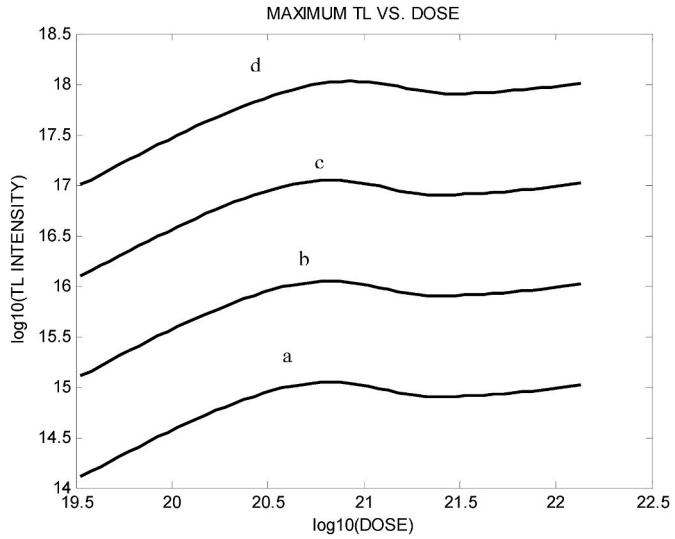

Fig. 7. Dependence of the dose dependence curve on the ratio M_2/M_1, on a log-log scale. M_1 remains the same as before being 3×10^{21} m^{-3}, and M_2(t) is the function given in Eq. (9) in curve (a); 10 times the function $M_2(t)$ in curve (b); 100 times $M_2(t)$ in curve (c) and 1000 times $M_2(t)$ in curve (d).

monotonically until it saturates with the value $n = N$. By conservation of charge, Eq. (14), it follows that m_1 does the same. The second step is to consider what happens to the free electron concentration, n_c. From Eq. (13), we see that n_c might, in general, either increase or decrease as n and m_1 increase. We have, however, chosen $A_n \approx 3A_{m1}$ and this assures that n_c increases as dose increases. Further, as n approaches saturation, $(N-n)$ approaches zero and the increase in n_c is quite sharp. This contrasts with the changes in n_v during irradiation. Because $m_1 \approx n$ and because we have chosen $M_1 \approx 3N$, the center population m_1 never approaches M_1. Consequently, the increase in n_v as dose increases is modest. After n saturates, meaning $n \approx N$, there is no further change in n or m_1 as dose increases and, consequently, n_c and n_v become constants. The third step is to consider how the rising free electron population, n_c, affects the concentration of the radiative center, m_2. From the initial conditions, Eq. (15), we know that m_2 starts at zero. This means that, initially, $m_{2QS} > m_2$ and, thus, from the conservation equation Eq. (20), it follows that m_2 initially increases as dose is applied. From Eq. (20), it follows that m_2 will continue to increase until m_2 reaches m_{2QS}. This is seen in Fig. 2. What happens next depends on how the value of m_{2QS} changes. From Eq. (22), we see that the value of m_{2QS} depends on n_c and n_v. Since, as discussed in the previous paragraph, before n saturates, n_c is rapidly increasing while n_v is relatively constant, it follows from Eq. (22) that m_{2QS} will decline until saturation of n is reached. From Eq. (20), this decline of m_{2QS} causes m_{2QS} to drop below m_2 which forces m_2 to decline. This is also seen in Fig. 2. After n saturates, $n \to N$, it follows from Eq. (13) that n_c and n_v become constant and, consequently, m_{2QS} becomes constant and remains so as dose increases. This is also apparent in Fig. 2. In sum, we have m_2 starting at zero and increasing as dose increases until it reaches the value m_{2QS}. At that point, m_2 reaches a peak and it declines thereafter as m_{2QS} declines. At very high doses, both m_{2QS} and m_2 approach a constant value. Since, as per Eq. (26), the value of the integrated thermoluminescence intensity is the value of m_2 after irradiation, it follows that, for this case of constant M_2, the integrated intensity also rises, reaches a peak, and then declines with increasing dose.

Now, let us consider the second case in which M_2 increases with dose. The first thing to notice is that if M_2 rises too fast, then, from Eq. (22), m_{2QS} will not decline. If m_{2QS} does not decline, then m_2 will be monotonic and we have lost the wiggle effect. Thus, it is important that the rate of increase of M_2 be below that point. With the rate of increase slow enough, m_2 will rise, reach a peak, and then, for a time, decline. As the dose increases further, n saturates and n_c and n_v approach constant values. Then, as per Eq. (22), the slowly rising value of M_2 will cause m_{2QS} to start rising again, as shown in Fig. 4. This, via Eq. (20), causes m_2 to start rising again, as also shown in Fig. 4. This means that the intensity again increases. This gives the full wiggle.

For both constant M_2 and increasing M_2, we have both solved the differential equations numerically and developed approximate analytical solutions. For the chosen parameters, both approaches found nearly identical results. It should be noted that one needs to convert between the dose as used in the model equations. While theoretical models typically measure the applied dose D in units of electron-hole pairs created per unit volume, experiments measure the applied dose D_{Gy} in units of energy deposited per unit mass with 1 Gy = 1 J/kg. The conversion between the two is (see e.g. Lawless et al., 2022)

$$D_{Gy} = \frac{W}{\rho} D, \tag{28}$$

where D_{Gy} is the dose in Gray, D the dose in m^{-3}, W (in *Joules*) is the average energy deposited per electron-hole pair created, and ρ (in kg/m^3) is the material mass density.

6. Conclusion

We have performed a theoretical study of two experimental phenomena previously reported in the literature. The first is the "conventional" non-monotonic dose dependence of TL, described by a curve which is initially an increasing function, reaching a maximum and then declines. We show that instead of the two-trap two-center model (Lawless et al. (2005) and Chen et al. (2006)), a model with one trap and two centers can be used. The second is a wiggly dose dependence in which the decline of intensity mentioned in the previous case is followed by another increase in intensity with dose, consequent from creation of radiative centers by irradiation. The full set of equations for both cases was solved by numerical simulation. An analytical solution was also developed and it provided an explanation for why these effects occur.

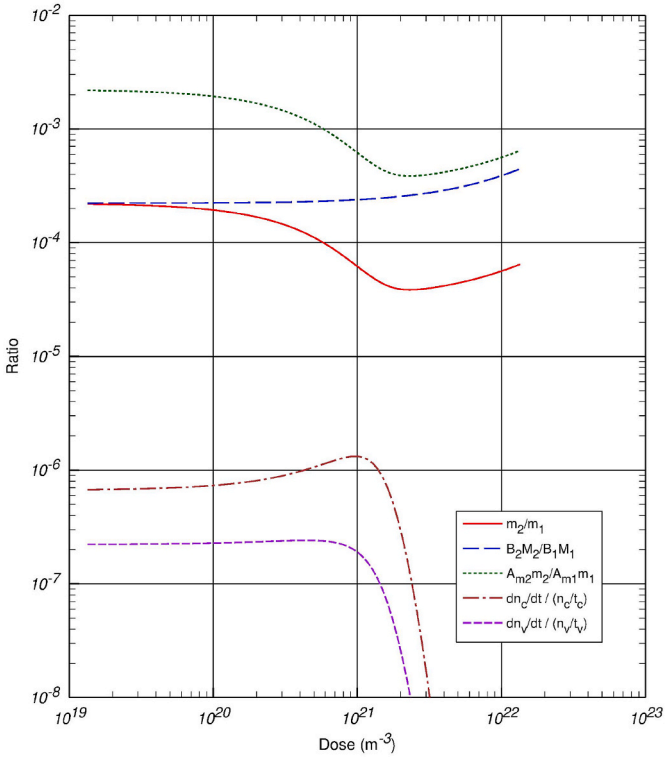

Fig. A1. The values of the functions m_2/m_1, $B_2M_2/(B_1M_1)$, $A_{m2}m_2/(A_{m1}m_1)$, $(dn_c/dt)/(n_c/t_c)$, and $(dn_v/dt)/(n_v/t_v)$ are plotted against the dose for the parameters used in the calculation of Fig. 4. To develop the analytical model, it was assumed that all these fractions were much less than one. The figure shows that those assumptions are valid.

CRediT authorship contribution statement

R. Chen: Writing – review & editing, Investigation, Conceptualization. **J.L. Lawless:** Writing – original draft, Validation, Software. **R. Arora:** Writing – original draft, Investigation.

Declaration of competing interest

The authors declare that they have no known competing financial interests or personal relationships that could have appeared to influence the work reported in this paper.

Data availability

Data will be made available on request.

Appendix

A. Validity of the simplifying assumption

A1. Small m_2

Three of the approximations that were used to simplify the governing equations required that the recombination center m_2 be small. Specifically (see Eq. (10)),

$$m_2 \ll m_1 \quad and \quad B_2M_2 \ll B_1M_1 \quad and \quad A_{m2}m_2 \ll A_{m1}m_1. \tag{A1}$$

Let us rewrite these approximations in the form of fractions that must be much less than one,

$$\frac{m_2}{m_1} \ll 1 \quad and \quad \frac{B_2M_2}{B_1M_1} \ll 1 \quad and \quad \frac{A_{m2}m_2}{A_{m1}m_1} \ll 1. \tag{A2}$$

For the parameters as used in Fig. 4, the values of these three fractions are shown, as function of dose, in Fig. A1. All the fractions are two to four orders of magnitude less than one, indicating that the approximations are well justified.

A2. The Quasi-steady approximation

For the quasi-steady approximation, we assumed

$$\frac{dn_c}{dt} \ll \frac{n_c}{t_c} \quad and \quad \frac{dn_v}{dt} \ll \frac{n_v}{t_v}, \tag{A3}$$

which are Eq. (12) above. Let us again rewrite them as fractions that must be less than one,

$$\frac{dn_c/dt}{n_c/t_c} \ll 1 \quad and \quad \frac{dn_v/dt}{n_v/t_v} \ll 1. \tag{A4}$$

These fractions are shown in Fig. A1. The fractions are six or more orders of magnitude less than one. This indicates that the quasi-steady approximations are quite accurate here.

References

Bargat, S.R., Parauha, Y.R., Mishra, G.C., Dhoble, S.J., 2020. Thermoluminescence study of $CaNa_2(SO_4)_2$ phosphor doped with Eu^{3+} and synthesized by combustion method. Luminescence 36, 1862–1868.

Burbidge, C.I., 2015. A broadly applicable function for describing luminescence dose response. J. Appl. Phys. 118, 044904.

Burbidge, C.I., Cabo Verde, S.I., Fernandes, A.C., Prudêncio, M.I., Botelho, M.L., Dias, M. I., Cardoso, G., 2011. Dosimetry in the multi kilo-Gray range using optically-stimulated luminescence (OSL) and thermally-transferred OSL from quartz. Radiat. Meas. 46, 860–865.

Burbidge, C.I., Dias, M.I., Prudêncio, M.I., Rebêlio, L.P., Cardoso, G., Brito, P., 2009. Internal α activity: localisation, compositional associations and effects on OSL signals in quartz approaching β saturation. Radiat. Meas. 44, 494–500.

Cameron, J.R., Suntharalingam, N., Kenney, G.N., 1968. Thermoluminescent Dosimetry. The University of Wisconsin Press, Madison, p. 60.

Charlesby, A., Partridge, R.H., 1963. The thermoluminescence of irradiated polyethylene and other polymers. Proc. Roy. Soc. A271, 170–187.

Chen, R., Lo, D., Lawless, J.L., 2006. Non-monotonic dose dependence of thermoluminescence. Radiat. Protect. Dosim. 19, 33–36.

Coreless, R.M., Jeffrey, D.J., 2002. The Wright ω function. In: Calmet, J., Benhamou, Caprotti, O., Henocque, L., Sorge, V. (Eds.), Artificial Intelligence, Automated Reasoning and Symbolic Computation. AISC Calculemus 2002. Lecture Notes in Computer Science, vol. 2385. Springer, Berlin, Heidelberg.

Halperin, A., Chen, R., 1966. Thermoluminescence in semiconducting diamonds. Phys. Rev. 148, 839–845.

Hughes, R.C., 1975. Electronic and ionic charge carriers in irradiated single crystal and fused quartz. Radiat. Eff. 26, 225–235.

Ichikawa, Y., 1968. Thermoluminescence of natural quartz irradiated by gamma rays. Japan. J. Appl. Phys. 7, 220–226.

Kalnins, C.A.G., Ebendorff-Heidenpriem, H., Spooner, N.A., Monro, T.M., 2012. Radiation dosimetry using optically stimulated luminescence in fluoride phosphate optical fibers. Opt. Mater. Express 2, 62–70.

Kortov, V., 2014. Modern trends and development in high-dose luminescent measurements. J. Phys.: Conf. Ser. 552, 012039.

Kortov, V., Pustovarov, V.A., Shtang, T.V., 2015. Radiation-induced transformations of luminescence centers in anion-defective alumina crystals under high-dose irradiations. NIMB 353, 42–45.

Lawless, J.L., Chen, R., Lo, D., Pagonis, V., 2005. A model for the non-monotonic dose dependence of thermoluminescence (TL). J. Phys. Condens. Matter 17, 737–753.

Lawless, J.L., Chen, R., Pagonis, V., 2022. Effect of radiation physics on inherent statistics of glow curves from small samples or low doses. Radiat. Meas. 151, 106698.

Lawless, J.L., Timar-Gabor, A., 2024. A new analytical model to fit both fine and coarse grained quartz. Radiat. Eff. 26, 225–235.

Lax, M., 1960. Cascade capture of electrons in solids. Phys. Rev. 119, 1502–1523.

Lewandowski, A.C., Mathur, V.K., 1996. High dose and phototransferred thermoluminescence in $CaSO_4$, $CaSO_4$:Dy, and $CaSO_4$:Tm. Radiat. Protect. Dosim. 66, 213–216.

Mathur, V.K., Lewandowski, A.C., Guardala, N.A., Price, J.L., 1999. High dose measurements using thermoluminescence of $CaSO_4$:Dy. Radiat. Meas. 30, 735–738.

Merezhnikov, A.S., Nikiforov, S.V., 2021. Non-monotonic dose dependence of thermoluminescence in spatially correlated systems. J. Lumin. 239, 118308.

Pagonis, V., Chen, R., Lawless, J.L., 2006. Non-monotonic dose dependence of OSL intensity due to competition during irradiation and readout. Radiat. Meas. 41, 903–906.

Pagonis, V., Kitis, G., Chen, R., 2020. A new analytical equation for the dose response of dosimetric materials, based on the Lambert W function. J. Lumin. 225, 117333.

Parauha, Y.R., Dhoble, S.J., 2020. Thermoluminescence study and evaluation of trapping parameters of rare earth activated $Ca_3Al_2O_6$:RE (RE=Eu^{2+}, Ce^{3+}) phosphors. J. Mol. Struct. 1211, 127993.

Sharma, G., Lochab, S.P., Singh, N., 2010. Investigation of thermoluminescence characteristics of CaSrS:Ce. Physica B 405, 4526–4529.

Prabhu, N.S., Sharmila, K., Somashekarappa, H.M., Lakshminarayana, G., Mandal, S., Sayyed, M.I., Kamath, S.D., 2020. Thermoluminescence features of Er^{3+} doped BaO-ZnO-LiF-B_2O_3 glass system for high-dose gamma dosimetry. Ceram. Int. 46, 19343–19353.

Sharma, K., Bahl, S., Singh, B., Kumar, P., Lochab, S.P., Pandey, A., 2018. $BaSO_4$:Eu as an energy independent thermoluminescent radiation dosimeter for gamma rays and C^{6+} ion beam. Radiat. Phys. Chem. 145, 64–73.

Yukihara, E.G., Whitley, V.H., Polf, J.C., Klein, D.M., McKeever, S.W.S., Akselrod, A.E., Akselrod, M.S., 2003. The effect of deep trap population on the thermoluminescence of Al_2O_3:C. Radiat. Meas. 37, 627–638.

Zahefidar, M., Eshraghi, L., Sadeghi, E., 2012. Thermoluminescence kinetics analysis of α-Al_2O_3:C at different dose levels and populations and a model for its dose response. Radiat. Meas. 47, 957–965.